diabetes®
American Diabetes Association®

Trefoil Factor 2 Expressed by the Murine Pancreatic Acinar Cells Is Required for the Development of Islets and for β-Cell Function During Aging

Jose A. Ortiz, Nadiah Ghazalli, Kassandra Lopez, Jeffrey Rawson, Erika M. McCown, Eunjin Oh, Jose M. Irimia, Kevin Jou, Jacob Mares, Min-Hsuan Chen, Xiwei Wu, Heather N. Zook, Janine C. Quijano, Neslihan Erdem, Anahy Lizarraga, Fouad Kandeel, Patrick T. Fueger, Debbie C. Thurmond, and Hsun Teresa Ku

Diabetes 2024;73(9):1447–1461 | https://doi.org/10.2337/db23-0490

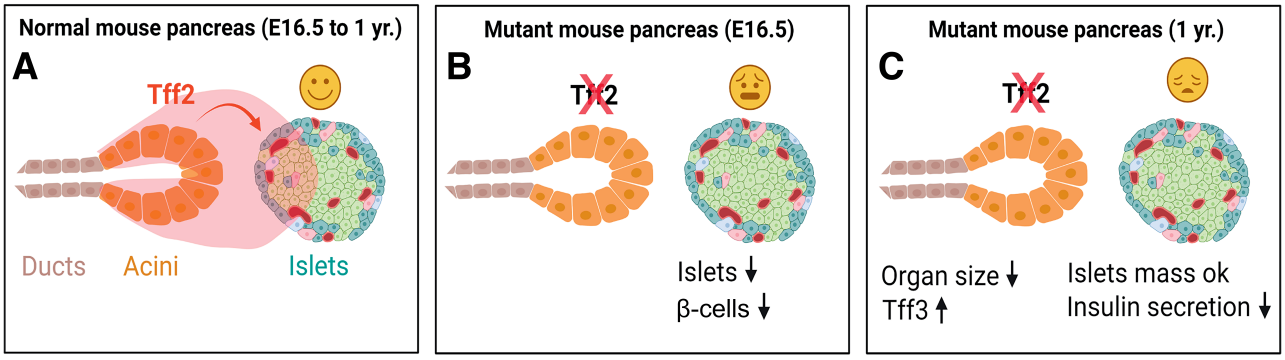

Trefoil Factor 2 Expressed by the Murine Pancreatic Acinar Cells Is Required for the Development of Islets and for β-Cell Function During Aging

Jose A. Ortiz,[1,2] Nadiah Ghazalli,[1,2] Kassandra Lopez,[2] Jeffrey Rawson,[1] Erika M. McCown,[3] Eunjin Oh,[3] Jose M. Irimia,[3,4] Kevin Jou,[1] Jacob Mares,[1] Min-Hsuan Chen,[5] Xiwei Wu,[4] Heather N. Zook,[1,2] Janine C. Quijano,[1] Neslihan Erdem,[1,2] Anahy Lizarraga,[6] Fouad Kandeel,[1] Patrick T. Fueger,[2,3,4] Debbie C. Thurmond,[2,3] and Hsun Teresa Ku[1,2]

Diabetes 2024;73:1447–1461 | https://doi.org/10.2337/db23-0490

Exocrine-to-endocrine cross talk in the pancreas is crucial to maintain β-cell function. However, the molecular mechanisms underlying this cross talk are largely undefined. Trefoil factor 2 (Tff2) is a secreted factor known to promote the proliferation of β-cells in vitro, but its physiological role in vivo in the pancreas is unknown. Also, it remains unclear which pancreatic cell type expresses Tff2 protein. We therefore created a mouse model with a conditional knockout of Tff2 in the murine pancreas. We find that the Tff2 protein is preferentially expressed in acinar but not ductal or endocrine cells. Tff2 deficiency in the pancreas reduces β-cell mass on embryonic day 16.5. However, homozygous mutant mice are born without a reduction of β-cells and with acinar Tff3 compensation by day 7. When mice are aged to 1 year, both male and female homozygous and male heterozygous mutants develop impaired glucose tolerance without affected insulin sensitivity. Perifusion analysis reveals that the second phase of glucose-stimulated insulin secretion from islets is reduced in aged homozygous mutant compared with controls. Collectively, these results demonstrate a previously unknown role of Tff2 as an exocrine acinar cell-derived protein required for maintaining functional endocrine β-cells in mice.

ARTICLE HIGHLIGHTS

- Exocrine-to-endocrine cross talk is important in maintaining pancreatic cell homeostasis, but the molecular mechanisms remain largely undefined.
- In the pancreas, the physiological role of the secreted factor Tff2 and the cell type that expresses Tff2 has been unclear.
- Pancreatic acinar cells are the major cell type expressing Tff2 protein, and specific loss of Tff2 in the pancreas reduces β-cells during development and attenuates glucose-stimulated insulin secretion during aging in conditional Tff2 knockout mice.
- Tff2 is a positive exocrine-produced factor required for the development and function of endocrine β-cells, which has implications in diabetes disease progression and therapy.

The pancreas contains exocrine and endocrine compartments, which secrete digestive enzymes and hormones that regulate blood glucose homeostasis, respectively. Dysfunction of the endocrine β-cells can result in type 1 or type 2 diabetes (T1D/T2D), which remains a global health concern (1). Increasing evidence indicates abnormalities in the exocrine pancreas impact β-cell function (2), such as cystic fibrosis (3,4), pancreatitis (5,6), and pancreatic cancer

[1]Department of Translational Research and Cellular Therapeutics, Arthur Riggs Diabetes and Metabolism Research Institute, City of Hope, Duarte, CA
[2]Irell and Manella School of Biological Sciences, Beckman Research Institute, City of Hope, Duarte, CA
[3]Department of Molecular & Cellular Endocrinology, Arthur Riggs Diabetes and Metabolism Research Institute, City of Hope, Duarte, CA
[4]Comprehensive Metabolic Phenotyping Core, City of Hope, Duarte, CA
[5]Integrative Genomics Core, City of Hope, Duarte, CA
[6]Eugene and Ruth Roberts Summer Student Academy, City of Hope, Duarte, CA
Corresponding author: Hsun Teresa Ku, hku@coh.org

Received 20 June 2023 and accepted 10 June 2024
This article contains supplementary material online at https://doi.org/10.2337/figshare.26018941.
This article is featured in a podcast available at diabetesjournals.org/diabetes/pages/diabetesbio.

(7,8), potentially through secreted factors. However, the exocrine cell-derived signaling factors that regulate β-cell function remain largely unknown.

The trefoil family of secretory peptides consists of three proteins: Tff1, Tff2, and Tff3. In adult murine pancreas, Tff2 (9) and Tff3 (10) but not Tff1 (11) are detected, and Tff2 is expressed at higher levels than Tff3 (12). Tff2 is conserved from birds to humans (13), and is highly resistant to denaturing conditions and enzymatic digestion due to the seven intramolecular disulfide bonds in its tertiary structure and compact quaternary structure (14). Tff2 is abundantly expressed in stomach (15,16) and immune cells (17), where it binds with mucins to form protective gastric mucus barriers (18) and regulates immune response (19,20). Additionally, Tff2 is expressed in the central nervous system (21,22), anterior pituitary (21), hypothalamus (23), and pancreas (12,24). When added exogenously in vitro, Tff2 promotes the proliferation of adult murine pancreatic β-cells (25) and rescues embryonic β-cell apoptosis (9). However, the physiological role of Tff2 in the pancreas has not been discerned. Furthermore, immunohistochemistry studies disagree on whether Tff2 is expressed by endocrine (25) or exocrine pancreas in mice (9). Thus, there is a critical need to clarify which compartment expresses Tff2.

Here, we generated a conditional Tff2 knockout mouse model to test the physiological requirement of Tff2 in the pancreas, and to clarify the expression pattern of Tff2. We find that Tff2 protein is preferentially expressed by adult murine pancreatic acinar cells, and that Tff2 deficiency results in reduced β-cell mass in the embryonic pancreas and impaired glucose tolerance (IGT) in aged mice. Our findings demonstrate previously unknown roles of Tff2 in the endogenous pancreas and implicate Tff2 as a key signaling factor mediating exocrine-to-endocrine crosstalk.

RESEARCH DESIGN AND METHODS

Mice and Maintenance

Experiments on mice were approved by the City of Hope Institutional Animal Care and Use Committee, Duarte, CA. All mice had a C57BL/6J genetic background, which harbors nicotinamide nucleotide transhydrogenase mutation (26) (Supplementary Fig. 1). The generation of *Pdx1:Cre;Tff2*$^{fl/fl}$ mice was achieved by intercrossing Pdx1:Cre mice (Jax #014647) with the Tff2 floxed (Tff2<tm1.1Htk> MGI: 7620295; *Tff2*$^{fl/fl}$) mice (see below).

Generation of Tff2 Floxed Mice

The mice harboring conditional knockout allele for Tff2 were designed and produced by Ozgene Pty Ltd. (Perth, Australia) (Supplementary Fig. 2).

Genotyping

PCR on genomic DNA with allele-specific primers (Supplementary Table 1) was used to determine genotypes.

Quantitative RT-PCR

Total RNA was isolated, converted into cDNA, and assayed using Taqman probes (Supplementary Table 2). β-Actin was used as the internal control.

Morphometric and Cell Quantification

Tile images from frozen and paraffin slides were collected, and then processed and quantified using QuPath v0.2.3 software.

Glucose-Stimulated Insulin Secretion

Static glucose-stimulated insulin secretion (GSIS) was performed as previously described (27). The levels of insulin release were adjusted based on total protein content and number of islets. Islet perifusion was conducted as previously described (28).

Statistical Analysis

Statistical significance was determined by unpaired, two-tailed Student *t* test when comparing two groups; Welch correction was used when comparing unequally sized samples. One-way ANOVA followed by Tukey post hoc analysis was used for comparing more than three groups. Data were analyzed with the GraphPad Prism 9 software and presented as mean ± SD or mean ± SEM.

Detailed methods are described in the Supplementary Material.

Data and Resource Availability

All data are available in the article or Supplementary Material. Data sets and resources are available from the corresponding author upon reasonable request.

RESULTS

Among the Trefoil Factor Family Members, *Tff2* Transcripts Are More Highly Expressed in Wild-Type Murine Pancreas Compared With *Tff3* and *Tff1*

Quantitative RT-PCR analyses revealed that *Tff2* was most expressed followed by *Tff3* and *Tff1* at embryonic day 16.5 (E16.5), postnatal day 0 (P0), P7, and 6 weeks (Fig. 1*A*). Consistent with a previous report (9), *Tff2* increased over time in the pancreas (Fig. 1*B*). Publicly available single-cell RNA-sequencing (scRNA-seq) databases indicate *Tff2* is expressed in trunk, acinar, endocrine progenitor, and endocrine cells at E15.5 and/or E18.5 (29) (Supplementary Fig. 3), and in adult acinar and ductal cells (12) (Supplementary Fig. 4). Because of this promiscuous gene expression pattern, we deleted *Tff2* in the whole pancreas.

Generation of Mice With *Tff2* Knockout in the Pancreas

We generated Tff2-floxed mice containing two loxP sites that flank exons 2 and 3 of the *Tff2* gene, which code for the trefoil domain necessary for Tff2 function (30), as

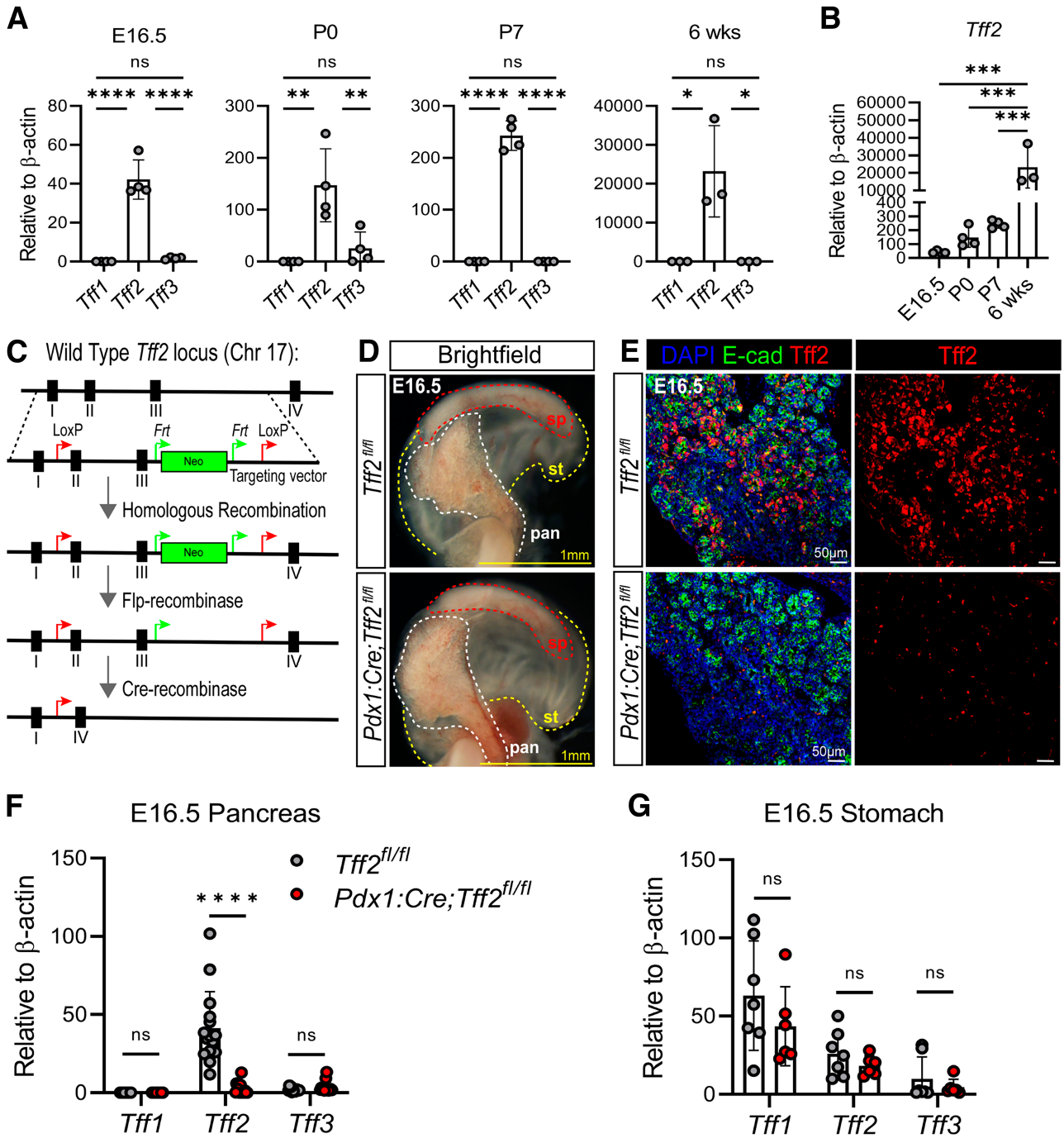

Figure 1—*Tff2* is expressed more highly than *Tff1* and *Tff3* in the wild-type murine pancreas and generation of a conditional Tff2 knockout mouse model. *A*: Conventional qRT-PCR analysis of *Tff1*, *Tff2*, and *Tff3* in pancreata collected at E16.5, P0, and P7, and 6 weeks old (6 wks). β-Actin was used as internal control; n = 3–4 pancreata. *B*: *Tff2* expression relative to β-actin increases over developmental time; n = 3–4 pancreata *C*: Schematic of generation of *Tff2* floxed mice (*Tff2* $^{fl/fl}$). Lox-P sites flanked exons 2 to 3, which allowed *Tff2* gene deletion after crossing with mice with Cre-recombinase expression (*Pdx1:Cre*). *D*: Representative brightfield images of E16.5 control (*Tff2* $^{fl/fl}$) and mutant (*Pdx1:Cre;Tff2* $^{fl/fl}$) pancreata (outlined with white-dashed lines; pan); st, stomach; sp, spleen. Scale bar = 1 mm. *E*: Co-IF staining of Tff2 (red) with E-cad (green) at E16.5 (n = 4–6 pancreata). Scale bar = 50 μm. *F* and *G*: Conventional qRT-PCR analysis of all Tffs relative to β-actin in the pancreas (*F*) and stomach (*G*) at E16.5 among mutant samples compared with controls (n = 14–15 for *F*, and n = 6–7 for *G*). Error bars represent SEM. *$P < 0.05$, **$P < 0.01$, ***$P < 0.001$, ****$P < 0.0001$ and not significant (ns) determined by one-way ANOVA with Tukey post hoc test for *A* and *B* and unpaired *t* test with Welch correction for *F* and *G*.

well as a Neo cassette flanked by two Frt sites inserted to the 5′ end of exon 3 (Fig. 1*C*). Subsequently, the Neo cassette was removed by crossing with Pgk1-Flp recombinase transgenic mice to generate the *Tff2* $^{fl/fl}$ mice, which were mated to transgenic Pdx1-Cre mice to delete *Tff2* in pancreatic cells (*Pdx1:Cre;Tff2* $^{fl/fl}$).

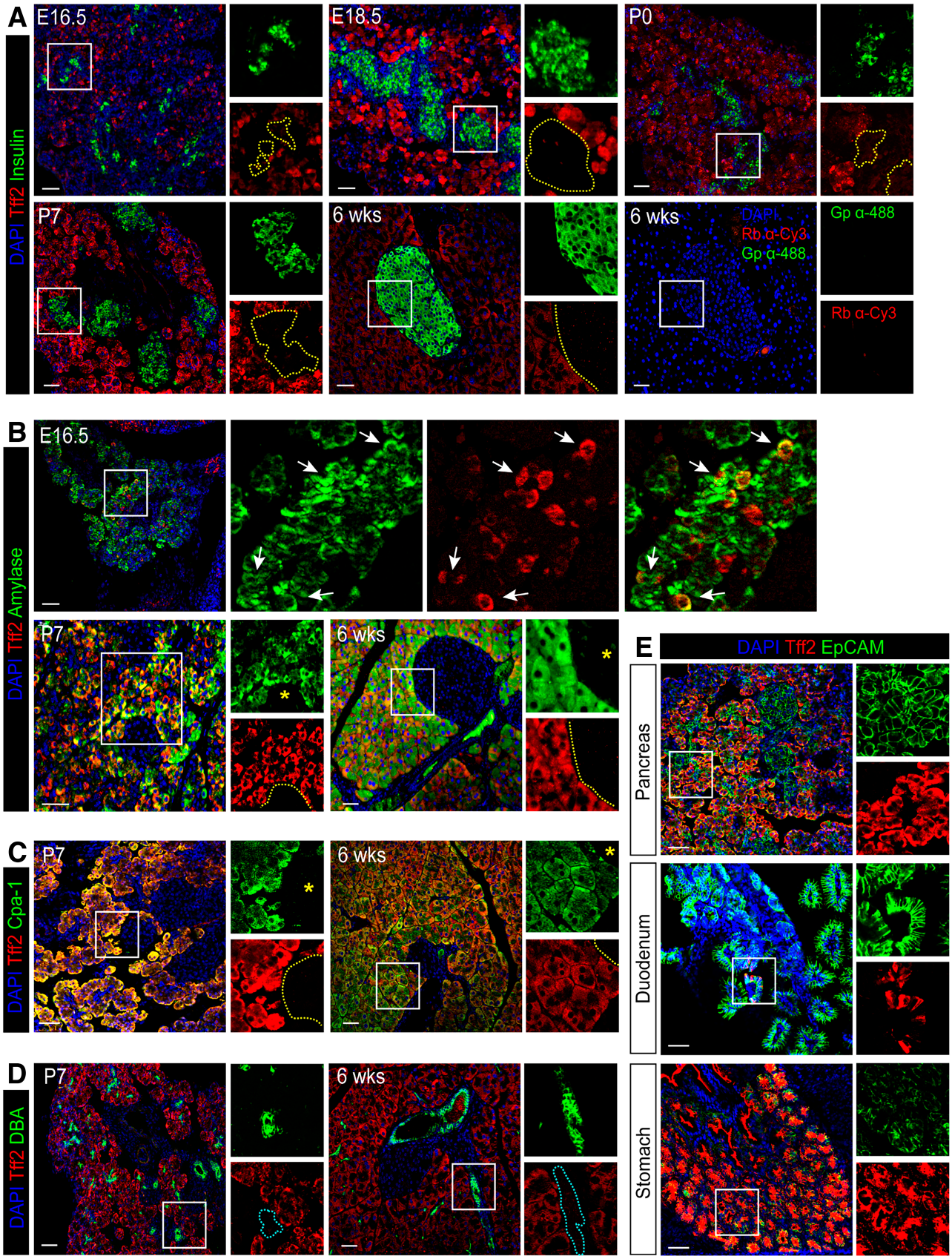

Figure 2—Tff2 protein is preferentially expressed by wild-type pancreatic acinar cells. *A*: Co-IF staining of Tff2 (red), insulin (green), and DAPI (blue) at E16.5, E18.5, P0, P7, and 6 weeks old (6 wks). Control tissue (6 wks, bottom right) treated with secondary antibodies only was used as negative control to adjust signal levels for Tff2. *B*: Co-IF staining of Tff2 (red), amylase (green), and DAPI (blue) at E16.5, P7,

Brightfield analysis of E16.5 embryos showed no observable differences in pancreas size and architecture between mutants and controls (Fig. 1*D* and Supplementary Fig. 5). Co-immunofluorescence (co-IF) staining of Tff2 and E-cadherin (E-cad, Cdh1) confirmed reduction of Tff2 protein in the pancreatic epithelium of mutants (Fig. 1*E*). Additionally, *Tff2* transcripts were reduced in the pancreas (Fig. 1*F*) but not in the stomach (Fig. 1*G*) of E16.5 mutants, confirming specificity. Furthermore, Tff2 protein in E16.5 stomach was maintained (Supplementary Fig. 6), but reduced in duodenum in mutants (Supplementary Fig. 6), as Pdx1 is expressed in both the duodenum and pancreas (31). Together, these results demonstrate that Tff2 is specifically reduced in the pancreas and duodenum.

Tff2 Protein Is Expressed in the Wild-Type Acinar but Not in β-Cells

To clarify Tff2 protein expression patterns, co-IF analyses revealed that Tff2 was absent in β-cells (Fig. 2*A*) and endocrine cells (Supplementary Fig. 7*A*). Instead, Tff2 colocalized with acinar cells (Fig. 2*B* and *C*) but not ductal cells (Fig. 2*D*). Colocalization of an epithelial cell marker (EpCAM) with Tff2 in P7 pancreas, duodenum, and stomach validated the specificity of the anti-Tff2 antibody (Fig. 2*E* and Supplementary Fig. 7*B* and *C*). Together, these results demonstrate that Tff2 protein is expressed preferentially in the murine acinar cells compared with β-cells or ductal cells.

Pancreatic Tff2 Knockout Alters a Broad Array of Gene Networks in E16.5 Embryos

To gain insights into the consequence of Tff2 knockout, genome-wide gene expression analysis was performed using bulk mRNA-sequencing (RNA-seq) on E16.5 pancreata. Multidimensional scaling analysis separated mutants from controls, suggesting distinct gene expression patterns (Supplementary Fig. 8*A*). A total of 1,143 differentially expressed genes (DEGs) were identified, with 695 upregulated and 448 downregulated (Fig. 3*A*, Supplementary Fig. 8*B*, and Supplementary Data Set 1). Gene set enrichment analysis (GSEA) of DEGs using Hallmark molecular signature database identified downregulated biological pathways: pancreatic β-cells, oxidative phosphorylation, and DNA repair (Fig. 3*B*). In contrast, upregulated pathways included epithelial mesenchymal transition, mitotic spindle, and G2M checkpoint (Fig. 3*B*). Another computational tool, Database for Annotation, Visualization and Integrated Discovery, identified downregulated biological processes in mutants, including peptide transport, hormone secretion, endocrine pancreas development, maturity onset diabetes of the young, and type II diabetes mellitus (T2D). Upregulated pathways in mutants included nervous system development, cell adhesion molecules, and phagosome (Supplementary Fig. 8*C* and *D*). These analyses suggest that early knockout of Tff2 impacts a wide range of biological processes in the embryonic pancreas.

Pancreatic Tff2 Deletion Reduces Endocrine and β-Cells in E16.5 Embryo

Because pancreatic β-cells was the most significant downregulated pathway in the mutant embryos (Fig. 3*B*), we examined endocrine marker expression. *Tff2* was the most downregulated gene (Fig. 3*C*), confirming the knockout. Many downregulated genes were known endocrine lineage markers, such as *Ins1*, *Ins2*, *Gcg*, *Ppy*, and *Sst* (Fig. 3*C*). Additional β-cell–related genes were also decreased in mutant pancreas samples, such as *Rfx6*, *Pax4*, *Pax6*, *Slc2a2*, *Iapp*, *Nkx6-1*, *Abcc8*, *Insm1*, and *Syt13* (Fig. 3*D*). qRT-PCR analysis confirmed the reduction of *Ins1*, *Ins2*, *Gcg*, *Ppy*, *Sst*, *Chga*, *Iapp*, *Abcc8*, and *G6pc2* in mutant pancreata (Fig. 3*E*). The co-IF staining revealed that the ratios of total endocrine cell ($Chga^+$) (Fig. 3*F* and *H*) and β-cell ($Insulin^+$) area to total pancreas area (Fig. 3*G* and *I*) were reduced in mutants. The pancreas area ($E\text{-}cad^+$) was not different between mutant and control embryos (Fig. 3*J*) nor was the percent sampling size (Supplementary Fig. 9). The ratio of ductal area (DBA^+) to total pancreas area was also not different (Fig. 3*K*). Together, these results demonstrate a loss of the endocrine compartment at E16.5 in response to Tff2 knockout.

Pancreatic Tff2-Deficient Mice Survive Birth and Have Tff3 Compensation at P7

Given the reduction in the embryonic β-cells at E16.5 (Fig. 3), we anticipated hyperglycemia in mutant mice after birth. Surprisingly, P7 mutant mice exhibited normal nonfasting blood glucose level, body weight, and pancreas weight (Fig. 4*A*–*C*). Mice were born in a Mendelian inheritance ratio with no observable changes in gross anatomy of the P7 mutant pancreas (Fig. 4*D*). Similar to E16.5, $Amylase^+$ acinar, DBA^+ ductal cells (Fig. 4*E*–*G* and Supplementary Fig. 10*A*), and pancreas area (Supplementary Fig. 10*B*) were not different in P7 mutants. However, unlike E16.5, the endocrine cells in P7 pancreas were no longer reduced in mutants (Fig. 4*H* and *I*). Also, no difference in $Ki67^+$ proliferating cells among mutant and control endocrine cells was observed (Fig. 4*J*).

Gene compensation is known to occur when mutations are deleterious (32). Given the similarities between the trefoil family proteins (14) and the known compensation of *Tff3* in the stomach of a Tff2 global knockout mouse model

and 6 wks. White arrows indicate $Tff2^+$ $amylase^+$ cells (yellow). *C*: Co-IF staining of Tff2 (red), Cpa-1 (green), and DAPI (blue) at P7 and 6 wks. *D*: Co-IF staining of Tff2 (red), DBA (green), and DAPI (blue) at P7 and 6 wks. *E*: Co-IF staining of Tff2 (red), EpCAM (green), and DAPI (blue) in P7 positive control tissues (pancreas, duodenum, stomach). Right panels show a ×4.9 magnification for *A* to *E* or ×13 magnification for *B* E16.5 or ×1.1 magnification for *B* P7 of the area marked by a white square. Yellow dotted lines and asterisk (*) outline islet/β-cell areas. Blue dotted lines outline ductal cell areas. Scale bar = 50 μm.

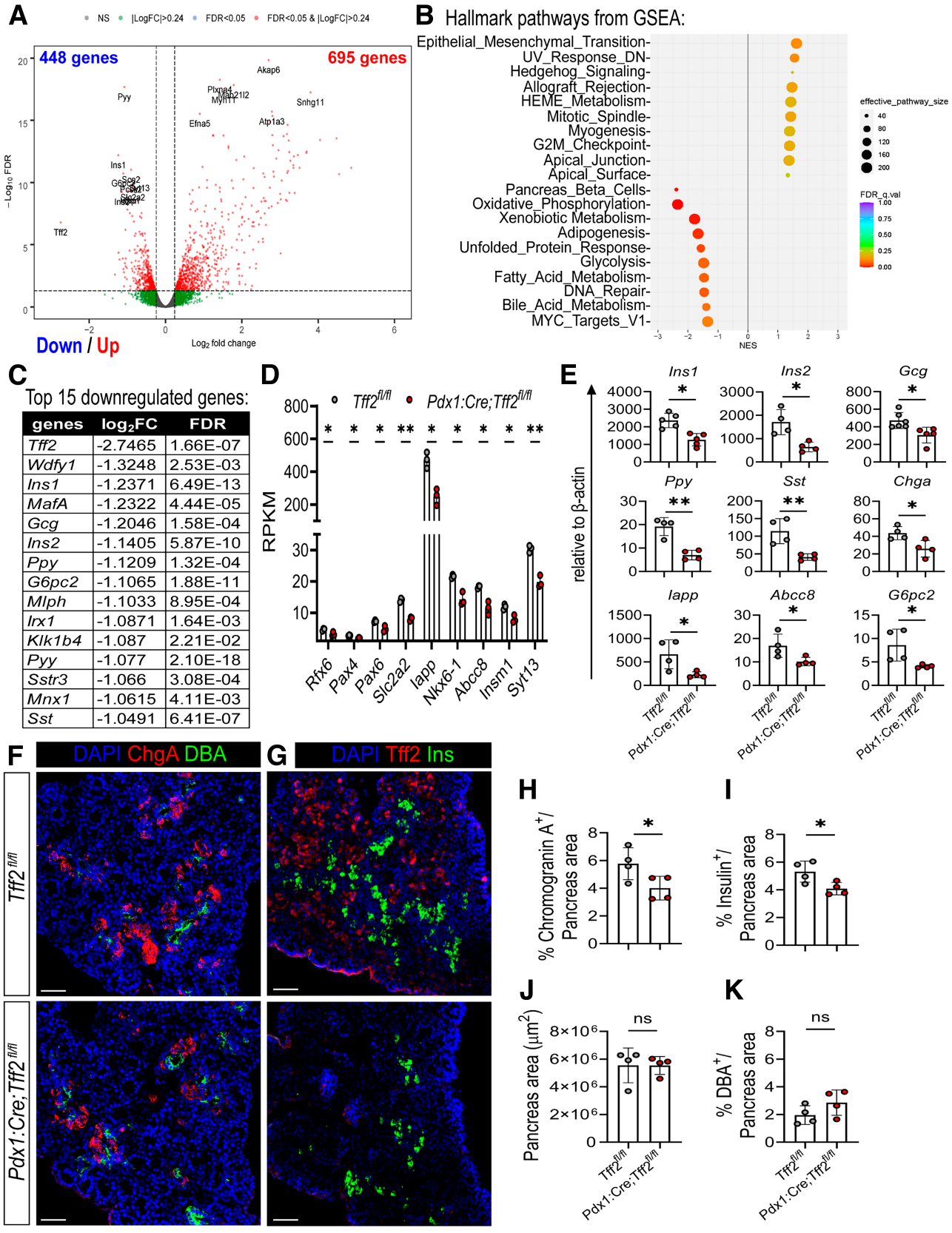

genes	log_2FC	FDR
Tff2	-2.7465	1.66E-07
Wdfy1	-1.3248	2.53E-03
Ins1	-1.2371	6.49E-13
MafA	-1.2322	4.44E-05
Gcg	-1.2046	1.58E-04
Ins2	-1.1405	5.87E-10
Ppy	-1.1209	1.32E-04
G6pc2	-1.1065	1.88E-11
Mlph	-1.1033	8.95E-04
Irx1	-1.0871	1.64E-03
Klk1b4	-1.087	2.21E-02
Pyy	-1.077	2.10E-18
Sstr3	-1.066	3.08E-04
Mnx1	-1.0615	4.11E-03
Sst	-1.0491	6.41E-07

Figure 3—Loss of Tff2 in the E16.5 pancreas leads to a reduction of islet and β-cells. *A*: Volcano plot showing a total of 1,143 DEGs in mutant compared with control pancreata at E16.5, with 448 downregulated and 695 upregulated DEGs (n = 3 pancreata per group). FC, fold change; FDR, false discovery rate. *B*: Hallmark pathways from GSEA. *C*: List of the top 15 downregulated DEGs. *D*: Reads per kilobase of transcript per million reads mapped (RPKM) levels of canonical pancreatic β-cell genes. *E*: Conventional qRT-PCR analysis of selected

(33), potential compensation by *Tff1* and/or *Tff3* in the mutant pancreas was examined. *Tff3,* but not *Tff1,* was upregulated in P7 mutant pancreas, and *Tff2* remained reduced (Fig. 4*K*). To further clarify, P7 pancreatic islets and exocrine tissues were separately examined: the only changes found were decreased *Tff2* and increased *Tff3* in the mutant exocrine compartment (Fig. 4*L*). IF staining confirmed the absence of Tff2 (Fig. 4*M*) and the presence of Tff3 protein (Fig. 4*N*) in the exocrine pancreas of P7 mutant mice. Antibody staining for Tff2 and Tff3 in positive control tissues confirmed specificity (Fig. 4*O* and Supplementary Fig. 10*C*).

Further examination of P0 pancreas revealed no difference in body weight, pancreas weight, gross anatomy, *Tff3* expression, endocrine pancreas area, proliferation of endocrine cells, or islet cell mass (Supplementary Fig. 10*D–N*). Together, these results indicate that early loss of Tff2 in the embryonic pancreas leads to recovery of endocrine cell mass by P0 and Tff3 compensation in acinar cells by P7.

Glucose Intolerance Develops in Pancreatic Tff2-Deficient Mice After Reaching 1 Year of Age

Despite Tff3 compensation in the pancreas of P7 mutant mice, we hypothesized that the loss of Tff2 may impact endocrine function because *1*) *Tff2* has a much higher (2,722 ± 797-fold; n = 3 each group; range 1,826–4,311) gene expression level compared with *Tff3* in 6-week pancreata (Fig. 1*A*), and *2*) *Tff2* transcript in acinar cells is found to be highest among 20 organs from adult mice in scRNA-seq analyses (12) (Supplementary Fig. 11). Therefore, homozygous (*Pdx1:Cre;Tff2*$^{fl/fl}$) and heterozygous (*Pdx1:Cre;Tff2*$^{fl/+}$) mutants and controls (*Tff2*$^{fl/fl}$) were monitored from 10 to 60 weeks of age. Body weight increased at 60 weeks for both male (Fig. 5*A* and Supplementary Fig. 12*A*) and female (Fig. 5*B* and Supplementary Fig. 12*B*) homozygous mutants compared with heterozygous and control mice. Fasting blood glucose levels were elevated >200 mg/dL at 40 weeks in male (Fig. 5*C*), but not female (Fig. 5*D*), homozygous mutant mice compared with heterozygous and control mice, suggesting females were protected. However, by 60 weeks, both male and female homozygous mutants had elevated fasting blood glucose compared with heterozygous mutants and controls (Fig. 5*C* and *D* and Supplementary Fig. 12*C* and *D*). Glucose tolerance, assayed by intraperitoneal glucose tolerance test (IP-GTT), was not different at 20 weeks of age (Fig. 5*E* and *F*). However, at 40 weeks, male (Fig. 5*G*) but not female (Fig. 5*H*) homozygous mutants became glucose intolerant, again indicating various degrees of impact by sex. By 60 weeks of age, male heterozygous mutants also became glucose intolerant (Fig. 5*I*), demonstrating Tff2 haplodeficiency impacts male mice. Female homozygous mutants also became glucose intolerant by 60 weeks (Fig. 5*J*).

To determine whether the glucose intolerance of mutant mice was due to insulin resistance, an intraperitoneal insulin tolerance test was performed. No difference was observed for both males and females (Supplementary Fig. 12*E* and *F*), indicating that insulin sensitivity in the peripheral tissues is conserved in homozygous and heterozygous mutant mice. Together, these results demonstrate the requirement of pancreatic Tff2 in maintaining glucose homeostasis during aging. Based on these results, we focused our attention on homozygous mutant male mice at ∼1 year of age in subsequent studies.

Pancreas Size Is Reduced in Aged Homozygous Mutant Mice Without Affecting Islet and β-Cell Mass

Decreased glucose clearance (Fig. 5*I* and *J*) with unchanged insulin sensitivity (Supplementary Fig. 12*E* and *F*) suggested a defect in β-cells in 1-year-old mutants. Tff2 knockout was first confirmed in acinar cells of homozygous mutants (Supplementary Fig. 13*A* and *B*). Surprisingly, pancreas weight and pancreas-to-body weight ratio were reduced for both mutant males (Fig. 6*A* and *B*) and females (Supplementary Fig. 13*C* and *D*).

To determine changes in islets, morphometric analysis was performed with a 5% sampling rate (Supplementary Fig. 13*E*). Hematoxylin and eosin staining (Fig. 6*C*) first confirmed that total pancreas area (Fig. 6*D*) and exocrine cell mass (Fig. 6*E* and Supplementary Fig. 13*F*) were reduced in male homozygous mutants. However, the islet-to-pancreas ratio (Supplementary Fig. 13*G*) and islet cell mass (Fig. 6*F*) were not different. Next, insulin colorimetric staining and morphometric analysis (Fig. 6*G*) revealed lowered total pancreas area (Fig. 6*H*) without changes in insulin-to-pancreas area ratio and β-cell mass (Fig. 6*I* and *J*) in mutant mice. Together, these results indicate that early loss of Tff2 perturbs pancreas size without altering islet and β-cell mass during aging.

Second-Phase Insulin Secretion Is Reduced in Islets From Aged Homozygous Mutant Male Mice

To determine changes in β-cell function, we isolated islets from aged male mice and performed an in vitro GSIS assay; islets were sequentially treated with low (2.8 mmol/L), high (20 mmol/L), and low concentrations of D-glucose, followed by 30 mmol/L KCl to stimulate maximal release of

endocrine cell genes relative to β-actin (n = 4–6 pancreata). Error bars represent SEM. *F* and *G*: Representative co-IF images from control (*Tff2*$^{fl/fl}$) and mutant (*Pdx1:Cre;Tff2*$^{fl/fl}$) embryos (E16.5) double-stained for Chromogranin A (ChgA: red) and DBA (green) (*F*) or Tff2 (red) and Insulin (green) (*G*) and DAPI (blue). Scale bar = 50 μm. *H–K*: Quantification of total islet, β, and ductal mass ratios relative to total pancreas area (10–16 sections 100 μm apart per pancreas, n = 4 pancreata). The ratio of total Chromogranin A$^+$ area (square micrometers) divided by total pancreas area (square micrometers) (*H*), the ratio of total insulin$^+$ area (square micrometers) divided by total pancreas area (square micrometers) (*I*), total pancreas area (square micrometers) (*J*), and the ratio of total DBA + area (square micrometers) divided by total pancreas area (square micrometers) (*K*) (n = 4 pancreata). Error bars represent SD. *P < 0.05, **P < 0.01 and not significant (ns) determined by two-tailed Student t test for *E* and *H–K* and unpaired t test with Holm-Šídák method for *D*.

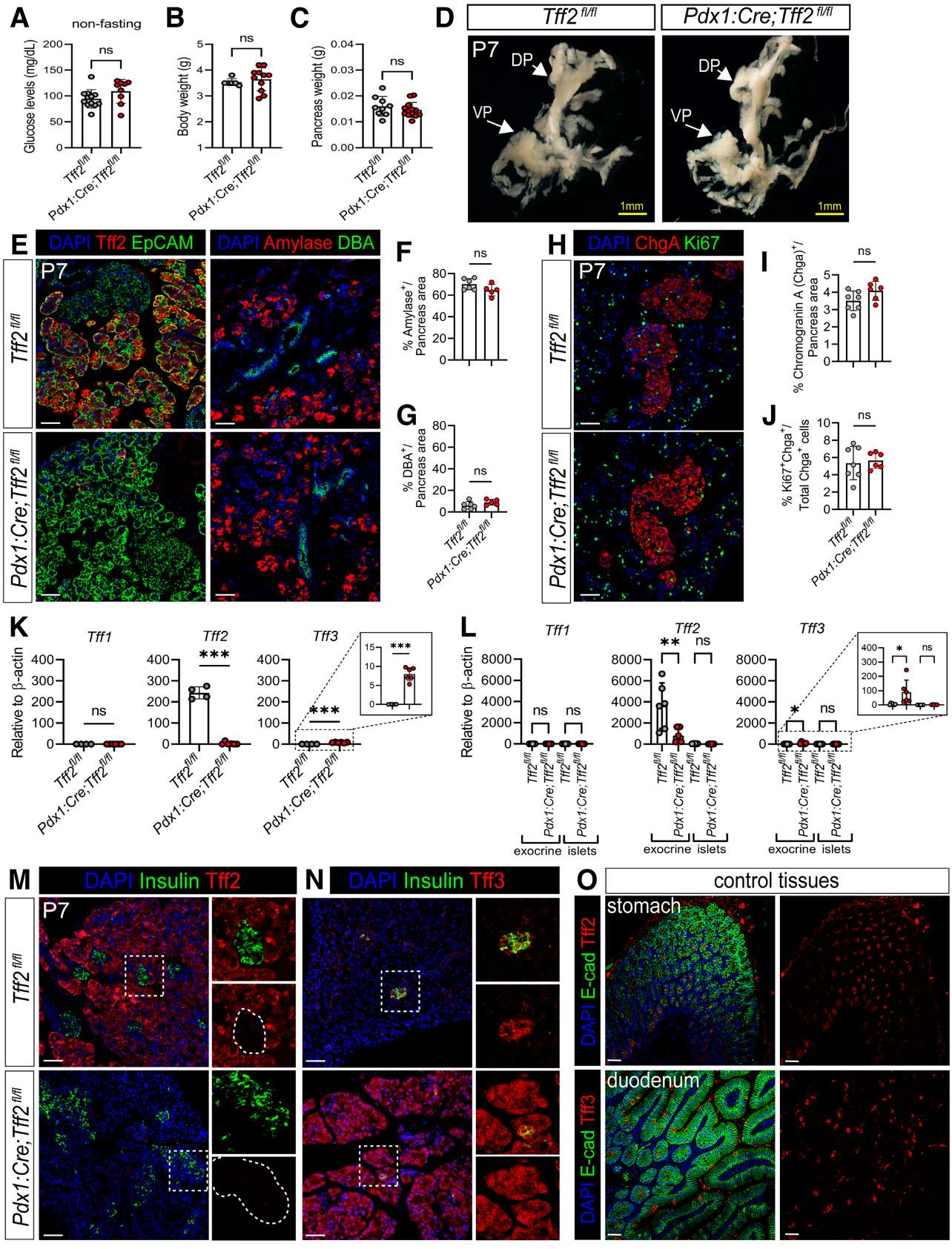

Figure 4—At P7, Tff3 is upregulated in the exocrine compartment in mutants compared with controls. *A–C*: Nonfasting blood glucose levels (*A*), body weight (*B*), and pancreas weight (*C*) at P7 (n = 6–13 mice). *D*: Representative brightfield images of dissected pancreata from control and mutant samples. Scale bar = 1 mm. *E*: Representative co-IF images from postnatal day 7 (P7) controls (*Tff2* $^{fl/fl}$) and mutants (*Pdx1:Cre;Tff2* $^{fl/fl}$) samples for Tff2 (red) and EpCAM (green) or amylase (red) and DBA (green). DAPI (blue) stains for nuclei. *F* and *G*:

insulin (Fig. 6*K* and *L*). As expected, islets isolated from control mice secreted more insulin in response to high glucose or KCl compared with low glucose (Fig. 6*L*, left). Islets from homozygous mutant mice also responded to high glucose or KCl, but the levels of insulin secreted were reduced (Fig. 6*L*, right). The protein content was not different between the mutant and control islets (Fig. 6*M*), indicating equivalent islet mass was used. These results indicate that static insulin secretion is impaired in the homozygous mutant islets.

To discern differences in insulin secretion dynamics, in vitro perifusion GSIS was performed. Insulin secretion was recorded every minute during glucose concentration changes, allowing quantification of the first and second phase of insulin secretion (Fig. 6*N*). As expected (28), control islets reached a peak in insulin secretion within 5 min of high-glucose stimulation, followed by a reduced yet sustained second phase that persisted in the presence of glucose (Fig. 6*N*). The areas under the curve (AUCs) for the first phase (14–20 min) trended lower but did not reach significance in the homozygous mutants (Fig. 6*O*, 1st phase). However, AUC of the second phase (22–45 min) was ∼45% lower in islets from homozygous mutants (Fig. 6*O*, 2nd phase), suggesting the recruitment of insulin granules from the internal storage pool is affected in β-cells. *Tff2* was reduced in the exocrine fraction post–islet isolation for the perifusion experiment (Fig. 6*P*, left), whereas *Tff3* expression remained higher in homozygous mutant exocrine fractions (Fig. 6*P*, right). Overall, these results suggest that loss of exocrine Tff2 impacts the second phase of insulin secretion in aged mouse β-cells.

Islets From Homozygous Mutant Male Mice Exhibit Reduced Melanophilin

To further characterize global gene expression changes in islets from homozygous mutants (n = 5 male mice, each group), bulk RNA-seq was performed. Surprisingly, only 22 DEGs were identified, with 15 genes upregulated and 7 genes downregulated (Fig. 7*A* and *B* and Supplementary Data Set 2). The exocrine fraction from homozygous mutant pancreata was confirmed to express lower levels of *Tff2* and higher levels of *Tff3* (Supplementary Fig. 14*A* and *B*). GSEA using Hallmark and Gene Ontology, Biological Processes molecular signature databases revealed downregulated pathways including protein secretion, Golgi vesicle transport, vesicle organization, establishment of protein localization to organelle, and vesicle localization (Fig. 7*C* and *D*). In contrast, upregulated pathways included TNFα signaling via NFκB, oxidative phosphorylation, glycolysis, cytoplasmic translation, inflammatory response, and leukocyte chemotaxis. This analysis suggests that reduced vesicle transport to the plasma membrane and increased metabolism and inflammatory response affects islets from homozygous mutant mice.

Melanophilin (*Mlph*) was identified as the most downregulated gene (Fig. 7*B*). Mlph in β-cells plays key roles in the second phase of insulin secretion (34). Co-IF analysis revealed that Mlph was coexpressed with insulin in aged control islets (Fig. 7*E*, top), as expected. However, aged mutant islets exhibited reduced Mlph expression among β-cells (Fig. 7*E*, bottom, and 7*F*). Together, these results demonstrate that the absence of pancreatic Tff2 correlates with reduced Mlph in aged β-cells.

DISCUSSION

In this study, we generated a conditional Tff2 knockout mouse model and demonstrated the critical physiological role of Tff2 in the pancreas. Because of Tff2's expression in multiple organs, investigating the pancreas in the global Tff2 knockout mice would have introduced confounding factors, especially from stomach, pituitary, and hypothalamus, which are known to participate in the metabolism of the whole body (35). We found that Tff2 loss in the pancreas resulted in a reduction of the endocrine compartment including the β-cells in E16.5 pancreas (Fig. 3). Upon reaching 1 year of age, homozygous mutant mice (both male and female) eventually developed glucose intolerance (Fig. 5) and showed defects in the second phase of GSIS (Fig. 6). Mutant males exhibited IGT much earlier than female mutants (Fig. 5), suggesting some impact by sex. This may be explained by the estrogen hormone produced by females that is known to protect against the development of metabolic syndrome, obesity, T2D, and insulin resistance in the C57BL/6 strain of mice (36).

Interestingly, endocrine mass recovered as early as P0 (Supplementary Fig. 10*N*), while Tff3 compensation in acinar was observed starting in P7 (Fig. 4*L*) and continued in 1-year-old homozygous mutant pancreas (Fig. 6*P*). These results suggest that Tff3 upregulation is not directly responsible for endocrine recovery prior to birth. However,

Quantification of total acinar (amylase$^+$) and ductal (DBA$^+$) cell mass ratios relative to total pancreas area (10–16 sections 100 μm apart per pancreas, n = 5–6 pancreata). *H*: Representative co-IF images for Chromogranin A (ChgA; red) and Ki67 (green). *I*: Quantification of total ChgA/total pancreas area ratio (10–16 sections 100 μm apart per pancreas, n = 6–7 pancreata). *J*: Quantification of total Ki67$^+$ ChgA$^+$ cells/total ChgA$^+$ cells (n = 5–6 pancreata). Error bars represent SD. *K*: Conventional qRT-PCR analyses of all Tffs relative to β-actin in dissected pancreata (n = 4–6 mice). *L*: Similar to *K*, but exocrine and islet fractions were separated and compared between mutant and control samples (n = 6 mice per group). Error bars represent SEM. *M* and *N*: Representative co-IF images from P7 samples double-stained for insulin (green) with Tff2 (red) (*M*) or Tff3 (red) (*N*). DAPI (blue) stains for nuclei. Right panels in *M* and *N* show ×4.1 magnification of the area marked by a white dotted square. Islet/β-cell areas in *M* are outlined by white dotted lines. *O*: Co-IF staining of control tissues using Tff2 (red) with E-cad (green) in stomach or Tff3 (red) with E-cad (green) in duodenum. DAPI (blue) stains for nuclei. $^*P < 0.05$, $^{**}P < 0.01$, $^{***}P < 0.001$ and not significant (ns) determined by two-tailed unpaired t test with Welch correction for *A–C*, *F*, *G*, and *I–L*. DP, dorsal pancreas; VP, ventral pancreas. Scale bar = 50 μm.

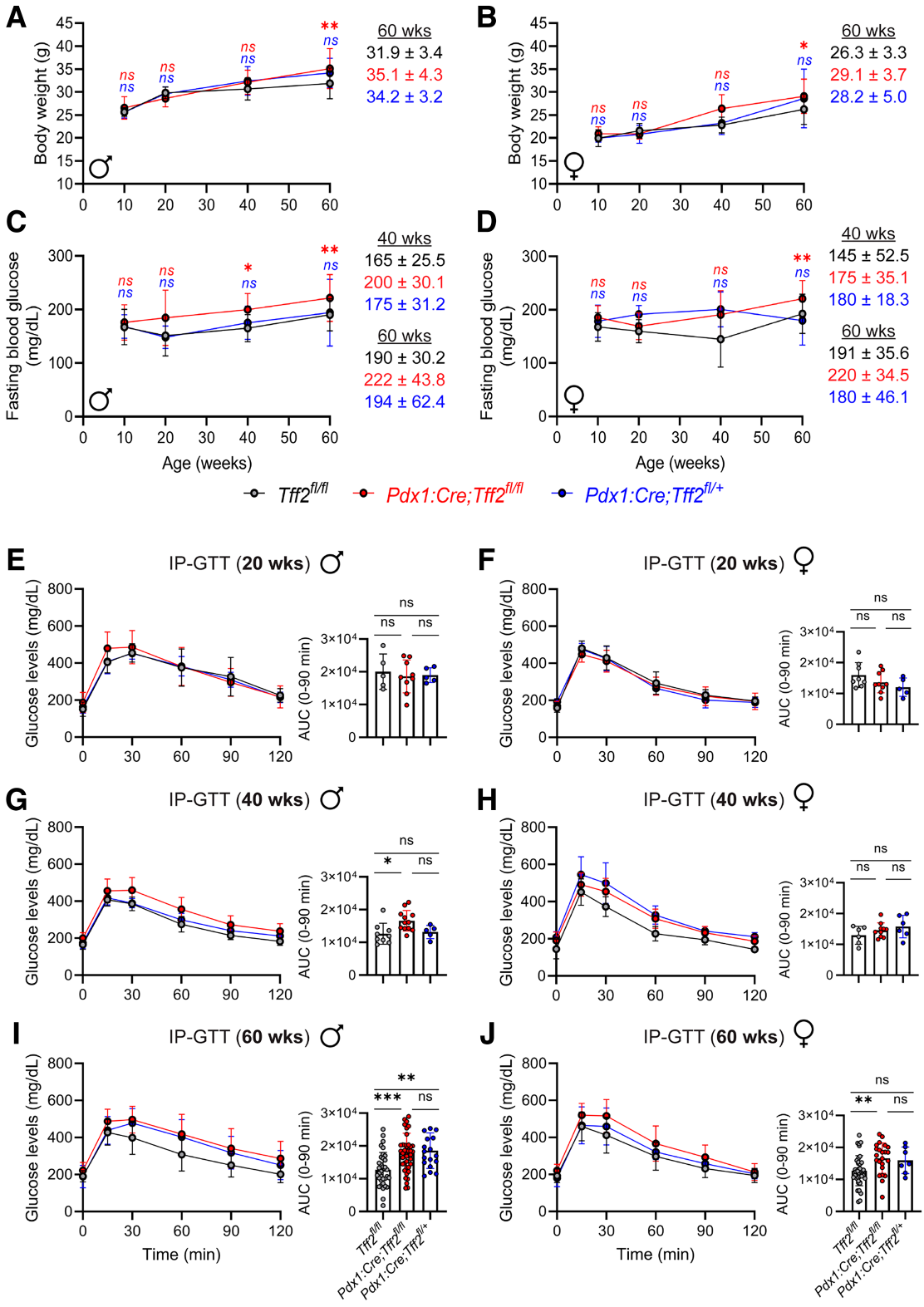

Figure 5—Upon reaching 1 year of age, homozygous mutant mice exhibit higher body weights and fasting blood glucose levels as well as IGT. *A* and *B*: The body weight of control (*Tff2*$^{fl/fl}$; black), heterozygous (*Pdx1:Cre;Tff2*$^{fl/+}$; blue), and homozygous (*Pdx1:Cre;Tff2*$^{fl/fl}$; red) male (*A*) and female (*B*) mice was monitored from 10 to 60 weeks (n = 5–41 for males, n = 5–40 for females). *C* and *D*: Blood glucose levels after a 6-h fasting period were monitored from 10 to 60 weeks of age for male (*C*) and female (*D*) cohorts (n = 5–41 for males, n = 3–40 for females). *E*–*J*: IP-GTT in male and female cohorts at 20 (*E* and *F*), 40 (*G* and *H*), and 60 weeks (*I* and *J*) (n = 5–41 for males, n = 5–40 for females). Right graphs in *E*–*J* depict quantification of the AUC from 0 to 90 min after intraperitoneal injection of D-glucose (2 g/kg body weight). Error bars represent SD. *$P < 0.05$, **$P < 0.01$, ***$P < 0.001$ and not significant (ns) determined by one-way ANOVA with Tukey post hoc test (*A*–*J*).

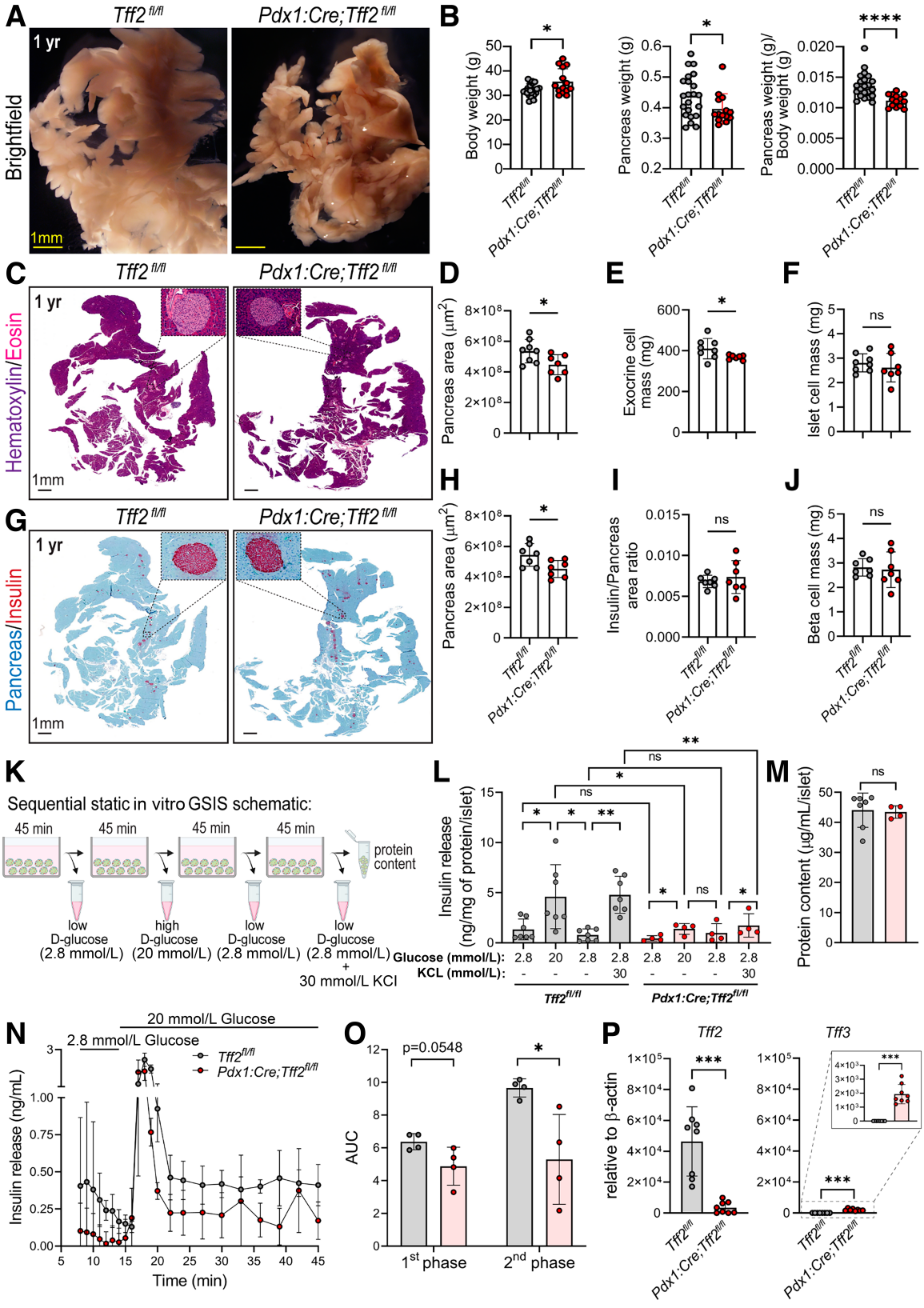

Figure 6—Aged homozygous mutants exhibit smaller pancreas organ size and impaired second-phase insulin secretion. *A*: Representative brightfield images of 1-year-old (1 yr) control (*Tff2* $^{fl/fl}$) and homozygous mutant (*Pdx1:Cre;Tff2* $^{fl/fl}$) pancreata. Scale bar = 1 mm. *B*: Body weight, pancreas weight, and pancreas-to-body weight ratio for aged males (n = 14–22 for males). Error bars represent SD. *C*: Representative photomicrographs of hematoxylin-eosin–stained aged control and mutant pancreata. Scale bar = 1 mm. *D–F*: Quantification of total pancreas area (square micrometers) (*D*), exocrine cell mass (*E*), and islet cell mass (*F*) (five to eight sections 100 μm apart

the upregulated Tff3 in acinar cells (Supplementary Fig. 10*N* and Fig. 4*L*) paired with the Tff3 in islet cells (Fig. 4*L* and *N*) may be sufficient to maintain glucose metabolism in mutant mice from P7 until 1 year of age because of Tff3's effects on β-cell proliferation (10) and insulin sensitivity (37).

Although endocrine cell mass was preserved, pancreas size was reduced in the aged homozygous mutant mice (Fig. 6), suggesting requirement of Tff2 in maintaining exocrine cell mass. This observation is echoed in a prior study by Kodama et al. where Pdx1 was specifically knocked down in acinar cells (38); these mice developed smaller exocrine pancreas and β-cell dysfunction. Interestingly, a follow-up study from the same group found that the smaller exocrine tissue was associated with reduced Tff2 (9). Our study provides causal evidence of Tff2 deficiency in exocrine size reduction. Pancreas weight and area was not changed at P0 (Supplementary Fig. 10*E* and *K*) or P7 (Fig. 4*C* and Supplementary Fig. 10*B*) in our mutant mice. Thus, pancreas size reduction occurs between P8 and 1 year, which can be influenced through proliferation in the exocrine pancreas during postnatal growth (P7–P28) (39), or a secondary effect of the lowered insulin trophic factor for acinar cells (40) from T1D or T2D islets (41,42).

We caution that Tff2 deficiency in the duodenum (Supplementary Fig. 6*B*) may contribute to body weight increase (Fig. 5) and pancreas size decrease (Fig. 6) in 1-year-old mutants. For example, duodenal ulcers can lead to weight gain due to postprandial pain relief (43), and duodenal obstruction may contribute to pancreatitis, affecting pancreas organ size (44). However, we did not observe morphological characteristics indicative of pancreatitis in aged mutants. Interestingly, our findings on weight gain differ from those reported by De Giorgio et al., who demonstrated that Tff2 null mice were protected from weight gain, because of increased energy expenditure and locomotor activity (23). This discrepancy may be attributed to confounding effects between global versus conditional Tff2 knockout mice.

Using co-IF staining, we clarified that Tff2 protein expression in the pancreas, between E16.5 and 6 weeks of age, is restricted to acinar cells (Fig. 2). Orime et al. demonstrated strong Tff2 protein expression in the islets of adult (10–14 weeks) murine pancreas (25). Using a different antibody, Hirata et al. showed Tff2 protein expression in the exocrine (both acinar and ductal cells) pancreas at E16.5, E18.5, and P1 (9); however, co-IF was not done to confirm lineage. We used the same commercially available antibody as Hirata et al., but with a higher dilution, and in combination with lineage markers. Hirata et al. further investigated the gene localization of *Tff2* using in situ hybridization, and found it expressed only in the acinar cells in 8-week-old pancreas (9). scRNA-seq analysis of 20 adult (10–15 weeks old) murine organs showed stronger expression of *Tff2* in pancreatic acinar compared with ductal cells (Supplementary Fig. 11*C*), and an absence of *Tff2* in islet cells (Supplementary Fig. 4*B*) (12). We found that *Tff2* was only expressed in the exocrine tissue (Fig. 4*L* and *M*). More recently, constitutive Tff2-Cre mice were generated that show embryonic lineage tracing to adult acinar but not endocrine or ductal cells (45). Notably, the aforementioned studies also utilized mice with C57BL/6 background, which indicates that the differences we observed in expression patterns were not due to strain differences. Taken together, we conclude that Tff2 is preferentially expressed by the exocrine acinar cells in the murine pancreas.

Transcriptomic analysis of aged islets from homozygous mutants versus control led to the identification of melanophilin (*Mlph*), a leading-edge gene in the vesicle localization pathway that is downregulated in mutants (Fig. 7*B* and *D*). Mlph functions in membrane trafficking, and, in skin, melanocytes form a complex with a GTPase, Rab27a, and myosin-Va on cortical actin filaments to direct the transfer of melanosomes (organelles that carry pigment) to the plasma membrane for secretion to neighboring keratinocytes (46). Mutations in *Mlph* cause problems with melanosome transportation that result in *leaden* (light-colored) mice compared with control mice with dark color (47). Additionally, *leaden* mice exhibit IGT due to reduced Mlph-associated insulin granule transportation to the plasma membrane during the second phase of insulin secretion (34,48). Our Tff2-deficient aged mice demonstrate the same reduction in the second phase of insulin secretion (Fig. 6*N* and *O*), which may be explained by the downregulation of Mlph (Fig. 7*B* and *F*). Future mechanistic

for each pancreas, n = 7–8 male mice). Error bars represent SD. *G*: Representative photomicrographs of immunohistochemistry staining of insulin (red) and hematoxylin (blue) in aged control and mutant pancreata. Scale bar = 1 mm. *H–J*: Quantification of total pancreas area (square micrometers) (*H*), the ratio of total insulin + area (square micrometers) divided by total pancreas area (*I*), and total β-cell mass (*J*) relative to total pancreas weight (five to eight sections 100 μm apart for each pancreas, n = 7 male mice). Error bars represent SD. *K* and *L*: In vitro GSIS in static incubation for cultured islets isolated from aged control and homozygous mutant male mice (n = 4–7). Error bars represent SEM. *M*: Protein content (*N*) of islets from *M* (n = 3–4 islet batches from four to seven male mice). Error bars represent SEM. *N*: Islets were isolated from aged male control or mutant mice and handpicked into groups of 40 and layered onto bead columns for parallel perifusion analysis. The islets were preincubated for 30 min in low glucose (2.8 mmol/L) followed by basal sample collection (1–13 min) to establish a baseline. Glucose was then elevated to 20 mmol/L for 35 min. Eluted fractions were collected at 1-min intervals at a flow rate of 0.3 mL/min, and secreted insulin was measured by radioimmunoassay. *O*: Quantification of the AUC for first-phase (14 to 20 min) and second-phase (22 to 45 min) insulin release from islets isolated from aged male control or mutant mice (n = 4 islet batches from eight male mice). Error bars represent SD. *P*: Conventional qRT-PCR analyses of *Tff2* and *Tff3* relative to β-actin in exocrine tissue fraction after islet isolation shown in *O* (n = 8 mice). Error bars represent SEM. $*P < 0.05$, $**P < 0.01$, $***P < 0.001$, $****P < 0.0001$ and not significant (ns) determined by two-tailed unpaired *t* test for *H–J*, *O*, and *P* or with Welch correction for *B*, *D–F*, *L*, and *M*.

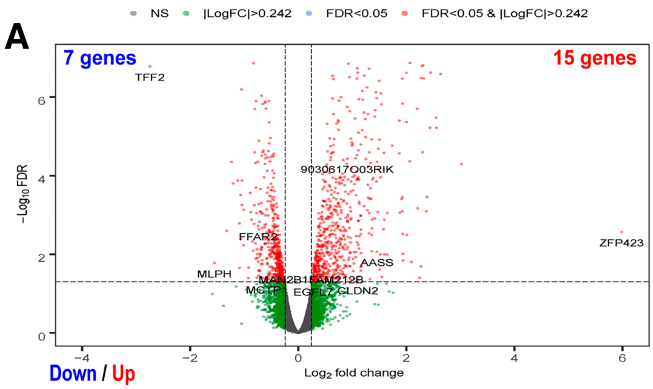

B Top downregulated genes:

genes	log_2FC	FDR
Mlph	-1.551	0.0167
Ffar2	-0.742	0.0019
Mctp1	-0.579	0.0429
Ppp1r10	-0.538	0.0027
Tmem229b	-0.285	0.0167
Man2b1	-0.272	0.0235
Thap2	-0.242	0.0451

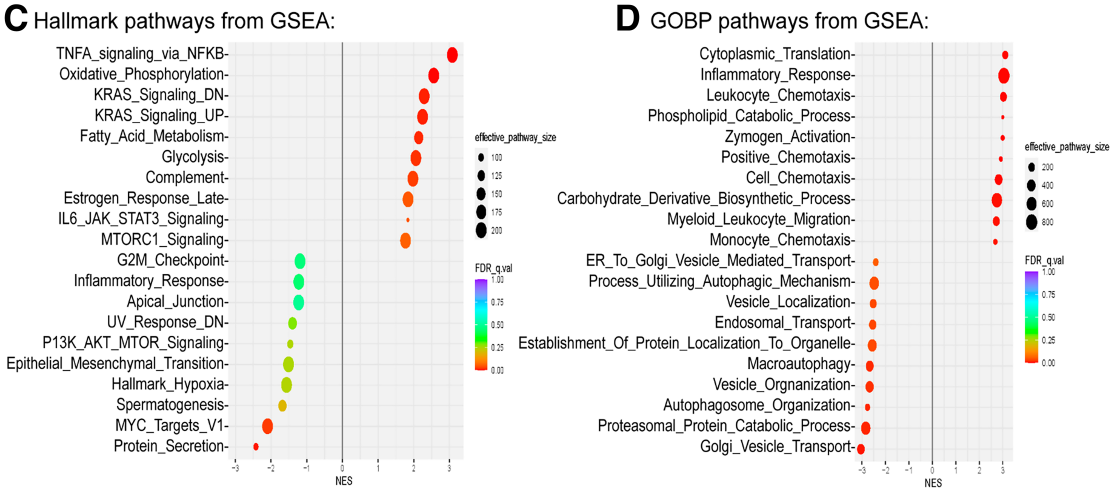

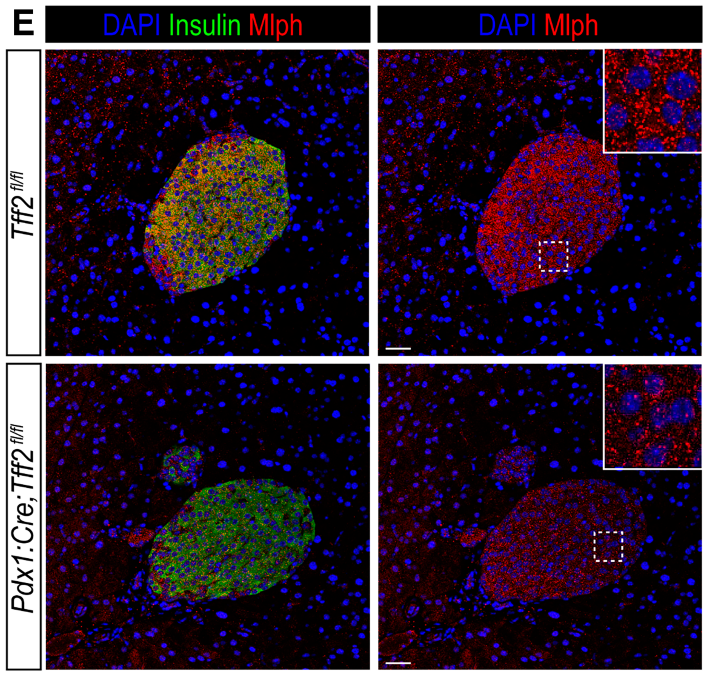

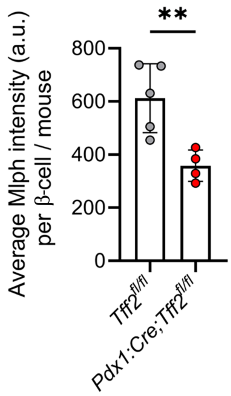

Figure 7— Melanophilin (Mlph) gene and protein are reduced in islets of homozygous mutants at 1 year of age. *A*: Bulk RNA-seq followed by volcano plot showing a total of 22 DEGs in aged homozygous mutant male pancreata compared with controls, with 7 downregulated and 15 upregulated genes ($n = 5$ each group). FC, fold change; FDR, false discovery rate. *B*: List of the seven downregulated DEGs (false discovery rate < 0.05). *C* and *D*: GSEA using Hallmark (*C*) and Gene Ontology, Biological Pathways (GOBP) (*D*) molecular signature databases. *E*: Representative co-IF images from aged control (*Tff2*$^{fl/fl}$) and mutant (*Pdx1:Cre;Tff2*$^{fl/fl}$) male mice pancreata stained with insulin (green), Mlph (red), and DAPI (blue). *F*: Quantification of Mlph protein signal intensities per individual β-cells per individual mouse ($n = 4$ mutant and 5 control male 1-year-old mice; $n = 3{,}589 \pm 1{,}356$ [range 1,949–5,800] β-cells per pancreas). Error bars represent SD. $^{**}P < 0.01$ determined by two-tailed unpaired *t* test with Welch correction. Right panels in *E* show a ×12.9 magnification of the area marked by a white dotted square ($n = 4$–5 each group). Scale bar = 50 μm.

studies are underway to clarify how the absence of Tff2 in the mouse pancreas leads to a downregulation of Mlph in aged β-cells. Interestingly, *Mlph* was also downregulated in the E16.5 mutants compared with controls (Fig. 3*C*), potentially through a different mechanism because E16.5 β-cells are not yet functional in GSIS (49).

Our results add to a growing number of studies that demonstrate that signals from the exocrine pancreas can affect the endocrine pancreas. For example, the risk of developing diabetes is increased by exocrine diseases, such as cystic fibrosis (3,4), pancreatitis (5,6), and pancreatic cancer (7,8). Also, patients with a mutation in an acinar-specific gene, carboxyl ester lipase, known as MODY8 gene, develop diabetes through secretion of the toxic mutant carboxyl ester lipase that is uptaken by the β-cells, causing dysfunction (50). Our study now identifies Tff2 as a beneficial protein, secreted from exocrine tissue, required for maintaining β-cell function.

In summary, we demonstrate that Tff2 is an exocrine regulator required for maintaining β-cell number during embryo development and sustaining β-cell secretory function during aging. Our finding has implications for diabetes disease progression and therapy.

Acknowledgments. The authors appreciate services provided by the following research cores at the City of Hope: Pathology, Light Microscopy Digital Imaging, Animal Resource Center, Integrative Genomics, and Comprehensive Metabolic Phenotyping. Some illustrations and the graphical abstract were created using BioRender.com.

Funding. Pathology, Light Microscopy Digital Imaging, Animal Resource Center, Integrative Genomics, and Comprehensive Metabolic Phenotyping are supported in part by the City of Hope Research Facilities grant P30CA033572 from the National Institutes of Health. J.A.O. received predoctoral fellowships from the Ford Foundation and from the Helen & Morgan Chu Fellowship at the Irell and Manella Graduate School of Biological Sciences. This project was supported in part by a City of Hope Arthur Riggs Diabetes & Metabolism Research Institute pilot grant and a grant from the National Institutes of Health, R01DK134652, to H.T.K., P.T.F., and D.C.T. Support from anonymous donor S.S. to H.T.K. is also gratefully acknowledged.

Duality of Interest. No potential conflicts of interest relevant to this article were reported.

The content is solely the responsibility of the authors and does not necessarily represent the official views of the National Institutes of Health.

Author Contributions. J.A.O. and H.T.K. conceived and planned the study. J.R., F.K., P.T.F., and D.C.T. provided key reagents. J.A.O., N.G., K.L., J.R., E.M.M., E.O., J.M.I., K.J., J.M., M.-H.C., X.W., H.N.Z., J.C.Q., N.E., and A.L. performed the experiments. J.A.O., J.M.I., J.M., M.-H.C., X.W., H.N.Z., J.C.Q., N.E., and H.T.K. performed the analyses. J.A.O., P.T.F., D.C.T., and H.T.K. interpreted data. J.A.O. and H.T.K. wrote the manuscript. J.A.O., J.M., H.N.Z., J.C.Q., P.T.F., D.C.T., and H.T.K. edited and revised draft manuscript. P.T.F., D.C.T., and H.T.K. acquired funding. H.T.K. is the guarantor of this work and, as such, had full access to all the data in the study and takes responsibility for the integrity of the data and the accuracy of the data analysis.

Prior Presentation. Part of this work was presented at the Society of Developmental Biology National Conference, virtual meeting, 14 July 2021, and the National Institutes of Health–National Institute of Diabetes and Digestive and Kidney Diseases Integrated Physiology of the Exocrine and Endocrine Compartments in Pancreatic Diseases Workshop, Bethesda, MD, 29–30 June 2022.

References

1. Saeedi P, Petersohn I, Salpea P, et al. Global and regional diabetes prevalence estimates for 2019 and projections for 2030 and 2045: Results from the International Diabetes Federation Diabetes Atlas, 9th edition. Diabetes Res Clin Pract 2019;157:107843

2. Rickels MR, Norris AW, Hull RL. A tale of two pancreases: exocrine pathology and endocrine dysfunction. Diabetologia 2020;63:2030–2039

3. Durie PR, Forstner GG. Pathophysiology of the exocrine pancreas in cystic fibrosis. J R Soc Med 1989;82:2–10

4. Kristidis P, Bozon D, Corey M, et al. Genetic determination of exocrine pancreatic function in cystic fibrosis. Am J Hum Genet 1992;50:1178–1184

5. Bhatia M, Wong FL, Cao Y, et al. Pathophysiology of acute pancreatitis. Pancreatology 2005;5:132–144

6. Pham A, Forsmark C. Chronic pancreatitis: review and update of etiology, risk factors, and management. F1000Res 2018;7:F1000 Faculty Rev-607

7. Woodmansey C, McGovern AP, McCullough KA, et al. Incidence, demographics, and clinical characteristics of diabetes of the exocrine pancreas (type 3c): a retrospective cohort study. Diabetes Care 2017;40:1486–1493

8. Hart PA, Bellin MD, Andersen DK, et al.; Consortium for the Study of Chronic Pancreatitis D, Pancreatic C. Type 3c (pancreatogenic) diabetes mellitus secondary to chronic pancreatitis and pancreatic cancer. Lancet Gastroenterol Hepatol 2016;1:226–237

9. Hirata K, Kodama S, Nakano Y, et al. Exocrine tissue-driven TFF2 prevents apoptotic cell death of endocrine lineage during pancreas organogenesis. Sci Rep 2019;9:1636

10. Fueger PT, Schisler JC, Lu D, et al. Trefoil factor 3 stimulates human and rodent pancreatic islet β-cell replication with retention of function. Mol Endocrinol 2008;22:1251–1259

11. Ebert MP, Hoffmann J, Haeckel C, et al. Induction of TFF1 gene expression in pancreas overexpressing transforming growth factor α. Gut 1999;45:105–111

12. Tabula Muris Consortium. Single-cell transcriptomics of 20 mouse organs creates a Tabula Muris. Nature 2018;562:367–372

13. Jiang Z, Lossie AC, Applegate TJ. Evolution of trefoil factor(s): genetic and spatio-temporal expression of trefoil factor 2 in the chicken (*Gallus gallus domesticus*). PLoS One 2011;6:e22691

14. Thim L, May FE. Structure of mammalian trefoil factors and functional insights. Cell Mol Life Sci 2005;62:2956–2973

15. Tomasetto C, Rio MC, Gautier C, et al. hSP, the domain-duplicated homolog of pS2 protein, is co-expressed with pS2 in stomach but not in breast carcinoma. Embo J 1990;9:407–414

16. Hanby AM, Poulsom R, Singh S, Elia G, Jeffery RE, Wright NA. Spasmolytic polypeptide is a major antral peptide: distribution of the trefoil peptides human spasmolytic polypeptide and pS2 in the stomach. Gastroenterology 1993;105:1110–1116

17. Cook GA, Familari M, Thim L, Giraud AS. The trefoil peptides TFF2 and TFF3 are expressed in rat lymphoid tissues and participate in the immune response. FEBS Lett 1999;456:155–159

18. Hoffmann W. Trefoil factor family (TFF) peptides and their diverse molecular functions in mucus barrier protection and more: changing the paradigm. Int J Mol Sci 2020;21

19. Baus-Loncar M, Schmid J, Lalani el N, et al. Trefoil factor 2 (TFF2) deficiency in murine digestive tract influences the immune system. Cell Physiol Biochem 2005;16:31–42

20. Kurt-Jones EA, Cao L, Sandor F, et al. Trefoil family factor 2 is expressed in murine gastric and immune cells and controls both gastrointestinal inflammation and systemic immune responses. Infect Immun 2007;75:471–480

21. Hinz M, Schwegler H, Chwieralski CE, et al. Trefoil factor family (TFF) expression in the mouse brain and pituitary: changes in the developing cerebellum. Peptides 2004;25:827–832

22. Hoffmann W, Jagla W. Cell type specific expression of secretory TFF peptides: colocalization with mucins and synthesis in the brain. Int Rev Cytol 2002;213:147–181
23. De Giorgio MR, Yoshioka M, Riedl I, et al. Trefoil factor family member 2 (Tff2) KO mice are protected from high-fat diet-induced obesity. Obesity (Silver Spring) 2013;21:1389–1395
24. Jorgensen KD, Diamant B, Jorgensen KH, Thim L. Pancreatic spasmolytic polypeptide (PSP): III. Pharmacology of a new porcine pancreatic polypeptide with spasmolytic and gastric acid secretion inhibitory effects. Regul Pept 1982;3:231–243
25. Orime K, Shirakawa J, Togashi Y, et al. Trefoil factor 2 promotes cell proliferation in pancreatic β-cells through CXCR-4-mediated ERK1/2 phosphorylation. Endocrinology 2013;154:54–64
26. Freeman HC, Hugill A, Dear NT, Ashcroft FM, Cox RD. Deletion of nicotinamide nucleotide transhydrogenase: a new quantitive trait locus accounting for glucose intolerance in C57BL/6J mice. Diabetes 2006;55:2153–2156
27. Huang C, Gu G. Effective isolation of functional islets from neonatal mouse pancreas. J Vis Exp 2017;119:55160
28. Oh E, Thurmond DC. Munc18c depletion selectively impairs the sustained phase of insulin release. Diabetes 2009;58:1165–1174
29. Krentz NAJ, Lee MYY, Xu EE, et al. Single-cell transcriptome profiling of mouse and hESC-derived pancreatic progenitors. Stem Cell Rep 2018;11:1551–1564
30. Farrell JJ, Taupin D, Koh TJ, et al. TFF2/SP-deficient mice show decreased gastric proliferation, increased acid secretion, and increased susceptibility to NSAID injury. J Clin Invest 2002;109:193–204
31. Guz Y, Montminy MR, Stein R, et al. Expression of murine STF-1, a putative insulin gene transcription factor, in beta cells of pancreas, duodenal epithelium and pancreatic exocrine and endocrine progenitors during ontogeny. Development 1995;121:11–18
32. Rossi A, Kontarakis Z, Gerri C, et al. Genetic compensation induced by deleterious mutations but not gene knockdowns. Nature 2015;524:230–233
33. Baus-Loncar M, Kayademir T, Takaishi S, Wang T. Trefoil factor family 2 deficiency and immune response. Cell Mol Life Sci 2005;62:2947–2955
34. Wang H, Mizuno K, Takahashi N, et al. Melanophilin accelerates insulin granule fusion without predocking to the plasma membrane. Diabetes 2020;69: 2655–2666
35. Gahete MD, Cordoba-Chacon J, Salvatori R, Castano JP, Kineman RD, Luque RM. Metabolic regulation of ghrelin O-acyl transferase (GOAT) expression in the mouse hypothalamus, pituitary, and stomach. Mol Cell Endocrinol 2010; 317:154–160
36. Shi H, Clegg DJ. Sex differences in the regulation of body weight. Physiol Behav 2009;97:199–204
37. Xue Y, Shen L, Cui Y, et al. Tff3, as a novel peptide, regulates hepatic glucose metabolism. PLoS One 2013;8:e75240
38. Kodama S, Nakano Y, Hirata K, et al. Diabetes caused by elastase-Cre-mediated Pdx1 inactivation in mice. Sci Rep 2016;6:21211
39. Houbracken I, Bouwens L. Acinar cells in the neonatal pancreas grow by self-duplication and not by neogenesis from duct cells. Sci Rep 2017;7:12643
40. Wright JJ, Williams JM, Letourneau-Freiberg LR, et al. Insulin deficiency from insulin gene mutation leads to smaller pancreas. Diabetes Care 2023;46: 773–776
41. Virostko J, Williams J, Hilmes M, et al. Pancreas volume declines during the first year after diagnosis of type 1 diabetes and exhibits altered diffusion at disease onset. Diabetes Care 2019;42:248–257
42. Garcia TS, Rech TH, Leitao CB. Pancreatic size and fat content in diabetes: a systematic review and meta-analysis of imaging studies. PLoS One 2017;12:e0180911
43. Wilcox CM, Clark WS. Features associated with painless peptic ulcer bleeding. Am J Gastroenterol 1997;92:1289–1292
44. Bansal A, Gupta P, Singh H, et al. Gastrointestinal complications in acute and chronic pancreatitis. JGH Open 2019;3:450–455
45. Jiang Z, Wu F, Laise P, et al. Tff2 defines transit-amplifying pancreatic acinar progenitors that lack regenerative potential and are protective against Kras-driven carcinogenesis. Cell Stem Cell 2023;30:1091–1109.e1097
46. Fukuda M, Kuroda TS, Mikoshiba K. Slac2-a/melanophilin, the missing link between Rab27 and myosin Va: implications of a tripartite protein complex for melanosome transport. J Biol Chem 2002;277:12432–12436
47. Matesic LE, Yip R, Reuss AE, et al. Mutations in Mlph, encoding a member of the Rab effector family, cause the melanosome transport defects observed in leaden mice. Proc Natl Acad Sci U S A 2001;98:10238–10243
48. Zhao K, Matsunaga K, Mizuno K, Wang H, Okunishi K, Izumi T. Functional hierarchy among different Rab27 effectors involved in secretory granule exocytosis. Elife 2023;12:e82821
49. Blum B, Hrvatin SS, Schuetz C, Bonal C, Rezania A, Melton DA. Functional beta-cell maturation is marked by an increased glucose threshold and by expression of urocortin 3. Nat Biotechnol 2012;30:261–264
50. Kahraman S, Dirice E, Basile G, et al. Abnormal exocrine-endocrine cell cross-talk promotes β-cell dysfunction and loss in MODY8. Nat Metab 2022; 4:76–89